

# Quantitative Analysis of Protein–Protein Interactions by Native Page/Fluorimaging

Kylie M. Wagstaff,<sup>1</sup> Manisha M. Dias,<sup>1</sup> Gualtiero Alvisi,<sup>1</sup> and David A. Jans<sup>1,2,3</sup>

Received February 17, 2005; accepted May 04, 2005

We have developed a new quantitative native PAGE mobility shift assay, which allows for the measurement of binding affinities for interacting protein pairs, one of which is fluorescently labelled. We have used it to examine recognition of the Simian virus 40 (SV40) large tumour T-antigen (T-ag) nuclear localisation sequence (NLS) by members of the importin (Imp) superfamily of nuclear transport proteins. We demonstrate that the T-ag NLS binds to the Imp  $\alpha/\beta$  heterodimer in NLS-dependent manner, determining that it binds with eight-fold higher affinity (340 nM), when compared to Imp  $\alpha$  alone, consistent with autoinhibition of Imp  $\alpha$  when not complexed with Imp  $\beta$ . The mobility shift assay is able to detect nM binding affinities, making it a sensitive and useful tool to analyse protein–protein interactions in solution.

**KEY WORDS:** Protein interactions; polyacrylamide gel electrophoresis; native PAGE mobility shift assay; importins; SV40 T-ag; nuclear localisation signal.

## INTRODUCTION

Quantitative analysis of protein–protein interactions can be complex and time consuming, usually involving the immobilisation of one or other of the interacting protein partners, e.g. in ELISA or biacore based approaches. We have devised a simple technique for quantifying the affinity of solution binding of two proteins under native conditions, one of which is fluorescently labelled, using native polyacrylamide gel electrophoresis (PAGE).

As applied here, native PAGE relies on the binding of an unlabelled protein to a fluorescently labelled protein, thus altering the shape/size of the protein, resulting in a shift in the mobility of the fluorophore during native PAGE. Our technique combines this with titration

of the unlabelled partner, and analysis of the digitised images obtained to determine the binding affinity of the interaction. As an example of one of the many applications of this assay, we present experiments measuring the binding affinity of proteins from the importin superfamily (Imp) to the nuclear localisation sequence (NLS) of the SV40 large tumour T antigen (T-ag) [1–3].

All transport into and out of a cell nucleus occurs via nuclear pore complexes (NPC) embedded in the nuclear envelope [3–5]. Active nuclear import is mediated by Imps [6,7] and requires the recognition of an NLS contained within the transport cargo protein [8,9]. In conventional nuclear import pathways, the NLS is recognised by the Imp  $\alpha/\beta$  heterodimer through the Imp  $\alpha$  subunit, followed by docking at the NPC mediated by the Imp  $\beta$  subunit [7,10]. Translocation into the nucleoplasm is followed by the binding of the monomeric guanine nucleotide binding protein Ran, in its GTP bound form, to Imp  $\beta$  to dissociate the complex [9,11]. Imp  $\beta$  facilitates the Imp  $\alpha$ -cargo interaction by binding to Imp  $\alpha$  and effecting a conformational change, which releases an autoinhibitory domain from the NLS binding site of Imp  $\alpha$ , thereby greatly increasing the affinity of the interaction

<sup>1</sup> Department of Biochemistry and Molecular Biology, Nuclear Signalling Laboratory, Monash University, Clayton, Australia.

<sup>2</sup> ARC Centre of Excellence for Biotechnology and Development, Canberra, Australia.

<sup>3</sup> To whom correspondence should be addressed at Nuclear Signalling Laboratory, Department of Biochemistry and Molecular Biology, Monash University, Clayton, VIC 3800, Australia. E-mail: david.jans@med.monash.edu.au

[12]. Importantly, this is also the basis of the cargo release step in the nucleus, where Imp  $\alpha$  dissociates from the NLS-containing protein as soon as Imp  $\beta$  is released through RanGTP binding.

As Imps form tight complexes with their transport cargoes they are ideal for use in this assay [4], which allows us to test for recognition by different Imps, as well as to quantify the strength of such interactions. It can also be applied to monitor the effects of protein modification on Imp binding.

## MATERIALS AND METHODS

The bacterial expression vector encoding GFP T-ag (102–135), containing the T-ag NLS (PKK<sup>128</sup>KRKV) was generated using the Gateway<sup>TM</sup> cloning technology (Invitrogen) essentially according to the manufacturer's instructions. Briefly, DNA fragments encoding T-ag (102–135) or the NLS mutant T-ag (102–135/Thr<sup>128</sup>), which contains threonine at position 128, flanked by attB recombination sites were generated by standard PCR techniques from templates L27 $\beta$ GAL or d10L27 $\beta$ GAL [13], respectively. These were recombined into the pDONR201 vector (Invitrogen) in a BP recombination reaction, and the resultant pDONR201-T-ag (102–135) or pDONR201-T-ag (102–135/Thr<sup>128</sup>) vectors recombined into pGFP-attC [14], a vector used to express GFP fusion proteins in bacteria, in the LR recombination reaction. The integrity of all expression constructs was verified by DNA sequencing.

GFP T-ag (102–135), GFP T-ag (102–135/Thr<sup>128</sup>) and GFP (alone) (expressed from plasmid pTRCA-EGFP [15]) were then purified from bacteria as hexa-histidine tagged proteins using nickel affinity chromatography under denaturing conditions, as done earlier [14,15]. The Imp proteins were purified from bacteria as GST-fusion proteins under native conditions as described [2,16–18]. A truncated variant of Imp  $\alpha$  (Tr- $\alpha$ ) [19], that lacks the autoinhibitory domain and is therefore able to bind to cargo with high affinity in the absence of Imp  $\beta$  was also expressed as a GST fusion protein as described. The Imp  $\alpha/\beta$  heterodimer was pre-dimerised at 13.6  $\mu$ M for 15 min at room temp for binding studies [14].

Native PAGE/Fluorimaging was performed by incubating 2  $\mu$ M fluorescently labelled protein with increasing amounts of Imp for 15 min at room temperature in a final volume of 25  $\mu$ l, made up with 1  $\times$  PBS (137 mM NaCl; 6.25 mM Na<sub>2</sub>HPO<sub>4</sub>; 2.5 mM NaH<sub>2</sub>PO<sub>4</sub>; pH 7.4). About 15  $\mu$ l of 40% sucrose was added and the samples run on pre-cast Tris-Glycine gels (either 8% or 4–20% gradient gels; Gradipore), under native conditions, in 1  $\times$  TBE (0.9 M Tris; 1.125 M boric acid; 20 mM EDTA, pH 7.5) at 80 V for 5 h at 4°C. Fluorescent bands were

visualised directly using the Wallach Arthur 1422 Multi-wavelength Fluorimager, using Excitation and Emission filters of 480/20 and 535/20 respectively, and exposure times of 1–3 s.

Fluorescent signals were measured by image analysis of the digitised images, using the ImageJ software (NIH). The percentage of protein with altered mobility due to complexation with Imps (shifted protein) in each lane was determined according to the formula:

$$\frac{(\text{Fluorescence of shifted band} - \text{Background fluorescence}) \times \text{Area of shifted band}}{(\text{Total fluorescence} - \text{Background fluorescence}) \times \text{Total area}}$$

where the total fluorescence represents the mean fluorescence in each lane (see Fig. 1(B), box a), the shifted fluorescence represents the mean fluorescence of the shifted band (Fig. 1(B), box b) and the background fluorescence represents the mean fluorescence of a region outside the fluorophore containing lanes (Fig. 1(B), box c). The percentage unshifted fluorescence was determined using the same equation, except that the mean fluorescence of the unshifted band (Fig. 1(B), box d) was substituted for that of the shifted band. Values were plotted against concentration using the Sigmaplot software and titration curves were fitted according to the formula  $y = a(1 - e^{-bx})$  or  $y = ae^{-bx}$  for the shifted and unshifted graphs respectively, from which the apparent dissociation constant ( $K_d$ ) could be calculated.

## RESULTS AND DISCUSSION

The T-ag NLS is known to be recognised with high affinity by the Imp  $\alpha/\beta$  heterodimer [3,20]. To validate our assay, the GFP T-ag (102–135) fusion protein was incubated with Tr- $\alpha$ , Imp  $\beta$  and  $\alpha/\beta$  (Fig. 1(A), *left panel*), with GFP alone as a control (Fig. 1(A), *right panel*). As expected a shift in mobility was observed for GFP T-ag (102–135) in the presence of Imp  $\alpha/\beta$ , through recognition of the NLS by the Imp  $\alpha$  subunit, demonstrated by the altered mobility observed with Tr- $\alpha$ . No shift in mobility was seen for GFP with any of the Imps, indicating that the observed interactions between Imps and GFP T-ag (102–135) are specific to the NLS.

Titration experiments were performed on GFP T-ag (102–135) (Fig. 1(B), *upper panel*) and the NLS mutated GFP T-ag (102–135/Thr<sup>128</sup>) derivative (Fig. 1(B), *lower panel*), with increasing concentrations of Imp  $\alpha/\beta$ . The NLS mutant had a significantly decreased affinity for Imp  $\alpha/\beta$ , requiring higher concentrations of Imps to generate the same shift in mobility when compared to the wild type protein. This emphasizes that altered mobility of the T-ag fusion protein is a direct result of its ability to bind to Imp  $\alpha/\beta$  with high affinity.

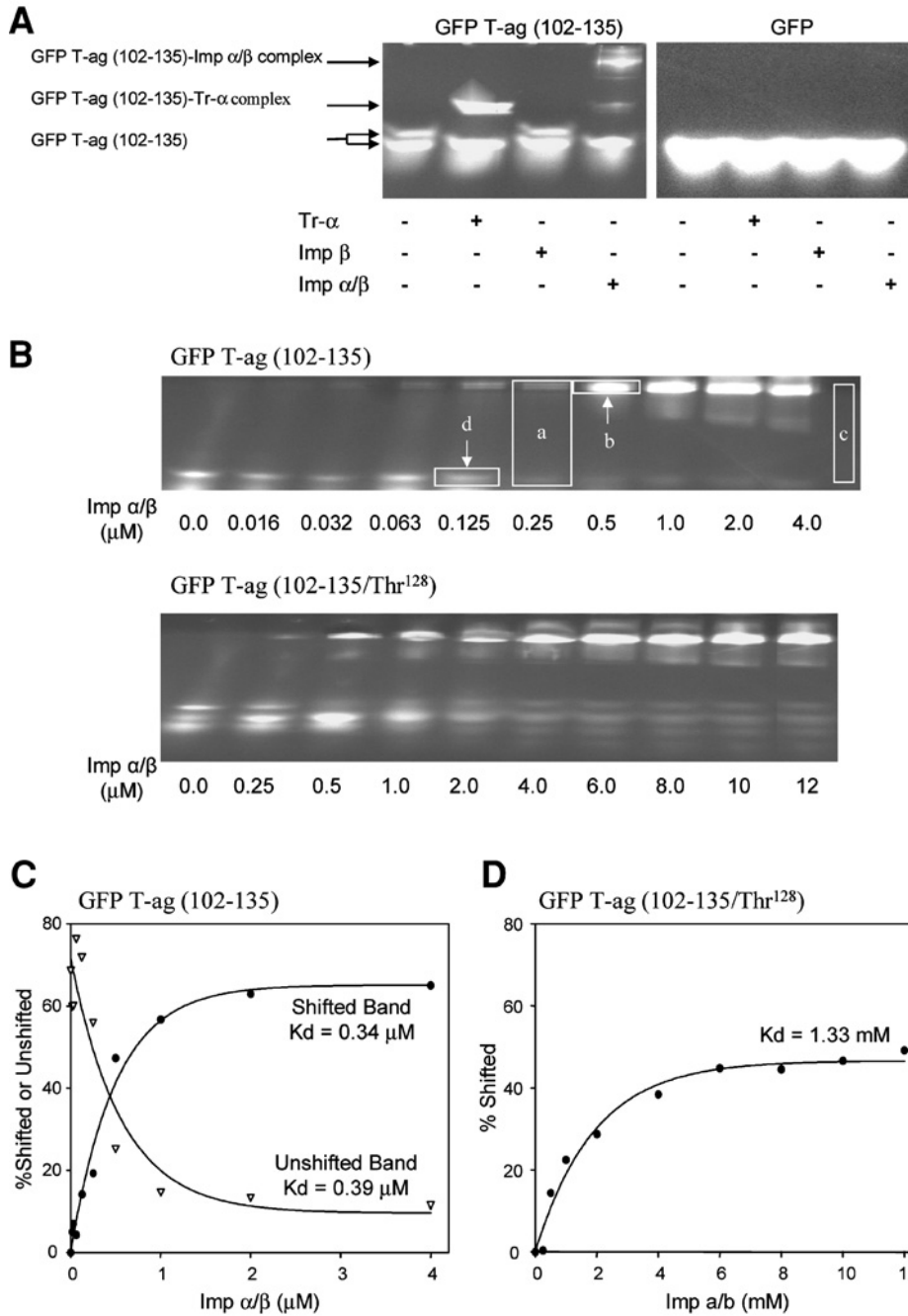


**Fig. 1.** NLS dependence of Imp binding to the T-ag NLS as shown by native PAGE/fluorimaging; evidence for autoinhibition of Imp  $\alpha$  (A)  $2 \mu\text{M}$  GFP T-ag (102–135) or GFP itself, were incubated either alone or with  $10 \mu\text{M}$  Tr- $\alpha$ , Imp  $\beta$  or Imp  $\alpha/\beta$  as indicated. (B) A  $2 \mu\text{M}$  GFP T-ag (102–135) (upper panel) or GFP T-ag (102–135/Thr<sup>128</sup>) (lower panel), were incubated with increasing concentrations of Imp  $\alpha/\beta$  as indicated. The image analysis approach is illustrated whereby a, b, c and d represent total, total shifted, background and total unshifted fluorescence respectively; measurements are made from areas such as those outlined by the white boxes. (C) Results of image analysis of the upper gel from B, used to determine the binding affinity of GFP T-ag (102–135) to Imp  $\alpha/\beta$ . Analysis was performed as described in materials and methods section and the binding curves generated were used to calculate the indicated dissociation constants ( $K_d$ ). (D) Results of image analysis of the lower gel such in B, performed as in C, to estimate a  $K_d$  for binding of GFP T-ag (102–135/Thr<sup>128</sup>) to Imp  $\alpha/\beta$ . (E) Results of image analysis of gels such as those in B, performed as in C, to estimate  $K_d$ s for binding of GFP T-ag (102–135) to Imp  $\alpha/\beta$  and  $\alpha$ .

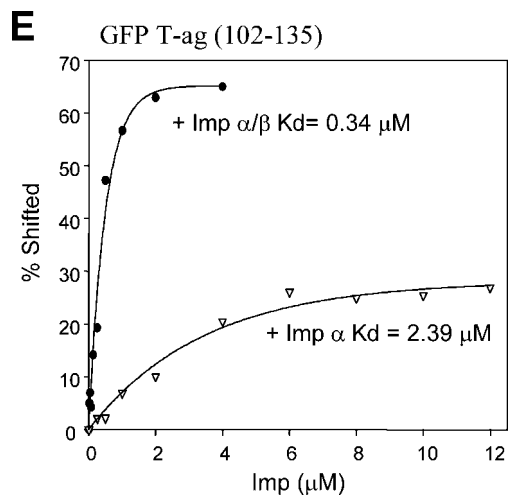


Fig. 1. Continued.

Image analysis of the titration experiments was performed to determine binding affinities of GFP T-ag (102–135) and its counterpart NLS mutant for Imp  $\alpha/\beta$ . Consistent with the qualitative assessment, GFP T-ag (102–135) binding to Imp  $\alpha/\beta$  has a  $K_d \sim$  four-fold lower than that for GFP T-ag (102–135/Thr<sup>128</sup>) ( $K_d = 0.34 \mu\text{M}$  vs.  $1.33 \mu\text{M}$  respectively, Fig. 1(C), (D)). Imp  $\alpha/\beta$  binding was also examined by analysing the unshifted bands, the results correlating well with those obtained from analysis of the shifted band (Fig. 1(C)). Utilising both these approaches, two  $K_d$  estimates are obtained from a single experiment, with highly reproducible results, highlighting the flexibility and power of this assay.

In identical fashion to the experiments above, native PAGE/Fluorimaging was performed on GFP T-ag (102–135) in the presence of increasing concentrations of Imp  $\alpha$  (Fig. 1(E)). Imp  $\alpha$  was found to recognise GFP T-ag (102–135) with high affinity ( $K_d = 2.4 \mu\text{M}$ ), but the  $K_d$  was eight-fold higher than for the Imp  $\alpha/\beta$  heterodimer, confirming that NLS recognition of GFP T-ag (102–135) by Imp  $\alpha$  requires Imp  $\beta$  for optimal binding affinity. Normally, the Imp  $\beta$  binding domain (IBB) of Imp  $\alpha$  is bound to the NLS binding site, causing autoinhibition. Upon binding of the IBB to Imp  $\beta$ , it is released from the NLS binding site, enabling high affinity interaction to occur [12], reflected in the eight-fold difference in binding affinity.

As demonstrated, this assay enables quick and efficient quantitation of the binding affinities for protein–protein interactions. The assay is a solution binding assay performed under native conditions, where neither protein is immobilised during the binding procedure, meaning that the proteins remain in their native conformation.

A similar gel mobility shift assay has been previously described [21]. This assay failed, however, to take into account background fluorescence, did not quantitate total fluorescence, and only generated one estimate of  $K_d$ . We have found that the consideration of both background and total fluorescence is critical for accurate estimation of binding constants, and as indicated, our assay generates two accurate  $K_d$  estimations (by analysing both shifted and unshifted protein fractions). Hence, our system has a number of advantages with respect to the reliability and reproducibility of the quantitation of the binding interactions. Most importantly, our assay can examine the binding of multi-subunit complexes, rather than only dimerisation [21].

Although it can be performed in standard gels, the assay optimally utilises pre-cast poly-acrylamide gels from Gradipore, which are contained in a transparent cassette. This means that the gels can be imaged directly in the cassette, minimising handling and exposure to acrylamide, and maximising the speed with which samples can be processed. Another significant benefit of this is the ability to image the gel more than once over time, as the gel can be run further if required. Other brands of pre-cast gels that have been trialled in this assay include those from Invitrogen<sup>TM</sup>, where imaging was not possible through the gel cassette, however. As the assay can determine the relative differences in binding affinities of proteins it can also be applied to examine post-translational modifications such as phosphorylation or acetylation.

## CONCLUSION

Native PAGE/fluorimaging can be used to examine a plethora of protein–protein interactions. The ability to quantitate the data means that subtle differences in binding affinities can be easily detected, such as those which result from protein modifications or mutations. Two estimates can be determined from the same experiment using the shifted and unshifted portions, making it a very powerful tool for measuring binding affinities in terms of reproducibility and flexibility. Due to the sensitivity of the assay, only  $\mu\text{M}$  amounts of protein are required and the fluorophore utilised can be varied to suit the desired application. Here we have shown only GFP-fusion proteins, but we have used the technique successfully with fluorescein-labelled proteins as well. In all, the assay represents a highly useful tool for quick and easy quantitative examination of physiological interactions in an *in vitro* setting.

## ACKNOWLEDGMENTS

The authors would like to acknowledge the support of the Australian National Health and Medical Research Council (fellowship #143790/#334013 and project grant #143710), and Anna Hearps for critical reading of the manuscript.

## REFERENCES

1. H. P. Rihs, D. A. Jans, H. Fan, and R. Peters (1991). The rate of nuclear cytoplasmic protein transport is determined by the casein kinase II site flanking the nuclear localisation sequence of the SV40 T-antigen. *EMBO J.* **10**(3), 633–639.
2. C. Y. Xiao, S. Hubner, and D. A. Jans (1997). SV40 large tumour antigen nuclear import is regulated by the double-stranded DNA-dependent protein kinase site (serine 120) flanking the nuclear localisation sequence. *J. Biologic. Chem.* **272**(35), 22191–22198.
3. E. Nigg (1997). Nucleocytoplasmic transport: Signals, mechanisms and regulation. *Nature* **386**, 779–787.
4. A. Harel and D. J. Forbes (2004). Importin beta: Conducting a much larger cellular symphony. *Mol. Cell.* **16**, 319–330.
5. S. Wente (2000). Gatekeepers of the nucleus. *Science* **288**, 1374–1377.
6. N. Mosammaparast and L. F. Pemberton (2004). Karyopherins: from nuclear transport mediators to nuclear function regulators. *Trends Cell Biol.* **14**, 547–556.
7. J. Moroiianu, G. Blobel, and A. Radu (1995). Previously identified protein of uncertain function is karyopherin alpha and together with karyopherin beta docks import substrate at nuclear pore complexes. *Proc. Natl. Acad. Sci. U.S.A.* **92**, 2008–2011.
8. D. A. Jans and S. Hubner (1996). Regulation of protein transport to the nucleus: central role of phosphorylation. *Physiologic. Rev.* **76**(3), 651–685.
9. Y. M. Chook, and G. Blobel (2001). Karyopherins and nuclear import. *Curr. Opin. Struct. Biol.* **11**, 703–715.
10. M. S. Moore (2003). Npap60: A new player in nuclear protein import. *Trends Cell Biol.* **13**(2), 61–64.
11. I. R. Vetter, C. Nowak, T. Nishimoto, J. Kuhlmann, and A. Wittinghofer (1999). Structure of a Ran-binding domain complexed with Ran bound to a GTP analogue: implications for nuclear transport. *Nature* **398**(6722), 39–46.
12. B. Kobe (1999). Autoinhibition by an internal nuclear localisation signal revealed by the crystal structure of mammalian importin alpha. *Nat. Struct. Biol.* **6**(4), 388–397.
13. H. P. Rihs and R. Peters (1989). Nuclear transport kinetics depend on phosphorylation-site-containing sequences flanking the karyophilic signal of the simian virus 40 T-antigen. *EMBO J.* **8**(5), 1479–1484.
14. B. Baliga, P. Colussi, S. Read, M. Dias, D. Jans, and S. Kumar (2003). Role of prodomain in importin-mediated nuclear localization and activation of caspase-2. *J. Biologic. Chem.* **278**(7), 4899–4905.
15. R. Lixin, A. Efthymiadis, B. Henderson, and D. A. Jans (2001). Novel properties of the nuclear targeting signal of human angiogenin. *Biochem. Biophys. Res. Commun.* **284**(1), 185–193.
16. S. Hubner, C. Y. Xiao, and D. A. Jans (1997). The protein kinase CK2 site (Ser111/112) enhances recognition of the simian virus 40 large T-antigen nuclear localisation sequence by importins. *J. Biologic. Chem.* **272**(27), 17191–17195.
17. S. Hubner, H. M. Smith, W. Hu, C. K. Chan, H. P. Rihs, B. M. Paschal, N. V. Raikhel, and D. A. Jans (1999). Plant importin alpha binds nuclear localization sequences with high affinity and can mediate nuclear import independent of importin beta. *J. Biologic. Chem.* **274**(32), 22610–22617.
18. A. Efthymiadis, H. Shao, S. Hubner, and D. Jans (1997). Kinetic characterization of the human retinoblastoma protein bipartite nuclear localization sequence (NLS) *in vivo* and *in vitro*. A comparison with the SV40 large T-antigen NLS. *J. Biologic. Chem.* **272**(35), 22134–22139.
19. B. Catimel, T. Teh, M. R. Fontes, I. G. Jennings, D. A. Jans, G. J. Howlett, E. C. Nice, and B. Kobe (2001). Biophysical characterization of interactions involving importin-alpha during nuclear import. *J. Biologic. Chem.* **276**(36), 34189–34198.
20. D. Calderon, W. D. Richardson, A. F. Markham, and A. E. Smith (1984). *Nature* **311**(5981), 33–38.
21. S. H. Park and R. T. Raines (1997). *Protein Sci.* **6**(11), 2344–2349.